

## Configuration-Dependent Interface Charge Transfer at a Molecule–Metal Junction

Li Wang, Lei Liu, Wei Chen, Yuanping Feng, and Andrew T. S. Wee\*

Contribution from the Department of Physics, National University of Singapore, Singapore 117542

Received March 13, 2006; E-mail: phyweets@nus.edu.sg

**Abstract:** The role of the molecule–metal interface is a key issue in molecular electronics. Interface charge transfer processes for 4-fluorobenzenethiol monolayers with different molecular orientations on Au(111) were studied by resonant photoemission spectroscopy. The electrons excited into the LUMO or LUMO+1 are strongly localized for the molecules standing up on Au(111). In contrast, an ultrafast charge transfer process was observed for the molecules lying down on Au(111). This configuration-dependent ultrafast electron transfer is dominated by an adiabatic mechanism and directly reflects the delocalization of the molecular orbitals for molecules lying down on Au(111). Theoretical calculations confirm that the molecular orbitals indeed experience a localization–delocalization transition resulting from hybridization between the molecular orbitals and metal surface. Such an orientation-dependent transition could be harnessed in molecular devices that switch via charge transfer when the molecular orientation is made to change.

### Introduction

Molecules have been shown to operate as Coulomb blockade structures,<sup>1</sup> diodes,<sup>2</sup> switching devices with high negative differential resistance (NRD),<sup>3</sup> and conductance switches,<sup>4</sup> making the nascent field of molecular electronics very promising. The central issue in molecular electronics is the characteristics of the molecule–metal interface, which strongly influences the transport properties in the molecular device.<sup>5</sup> Several factors, such as the geometry of the contacts,<sup>6–8</sup> bonding,<sup>7,9–10</sup> molecule–electrode distance,<sup>7,11,12</sup> and molecular orientation,<sup>13,14</sup> have been found to strongly affect the transport process. It remains a challenge to experimentally determine the role of the molecule–metal interface on the transport process, and most published work has been largely theoretical calculations.<sup>15</sup> Moreover, the electron transfer process across the molecule/electrode junction is still poorly understood,<sup>16</sup> and

problems related to this topic, such as the dynamics of electron transfer and the transfer mechanism, remain unresolved.

Resonant photoemission spectroscopy (REPES) provides a feasible tool to characterize the electronic structure of molecular monolayers.<sup>17–19</sup> REPES is also able to monitor ultrafast electron transfer in the femtosecond<sup>20</sup> or attosecond time scales.<sup>21</sup> In REPES experiments, electrons in a particular core level (the C 1s core level in our case) are first photoexcited by soft X-ray photons to a resonant-bound state with the system remaining charge neutral (this process is known as X-ray absorption, as shown in Figure 1a); this is followed by the deexcitation of the system via predominantly Auger-like transitions. If the excited electrons are localized at an excited orbital for a sufficiently long lifetime, two new transitions are possible: resonant Auger transition, where the final state has two holes left in the HOMOs and one excited electron in the LUMOs, as shown in Figure 1b, or resonant photoemission (Figure 1c), where the final state has one hole left in the HOMOs and is in an energetically equivalent final state as normal valence band photoemission.<sup>22</sup> If the molecular orbitals are strongly coupled to the support (Au single crystal in our case), as shown in Figure 1d, there is the possibility of interface charge transfer, in which the excited electrons directly decay into the Au conduction band and the core hole decays via a normal Auger process leaving a two-

- (1) Reed, M. A.; Zhou, C.; Muller, C. J.; Burgin, T. P.; Tour, J. M. *Science* **1997**, *278*, 252.
- (2) Wong, E. W.; Collier, C. P.; Behloradsky, M.; Raymo, F. M.; Stoddart, J. F.; Heath, J. R. *J. Am. Chem. Soc.* **2000**, *122*, 5831.
- (3) Chen, J.; Reed, M. A.; Rawlett, A. M.; Tour, J. M. *Science* **1999**, *286*, 1550.
- (4) Donhauser, Z. J.; Mantoosh, B. A.; Kelly, K. F.; Bumm, L. A.; Monnell, J. D.; Stapleton, J. J.; Price, D. W.; Rawlett, A. M.; Allara, D. L.; Tour, J. M.; Weiss, P. S. *Science* **2001**, *292*, 2303.
- (5) Kushmerick, J. G.; Holt, D. B.; Yang, J. C.; Naciri, J.; Moore, M. H.; Shashidhar, R. *Phys. Rev. Lett.* **2002**, *89*, 086802.
- (6) Yaliraki, S. N.; Ratner, M. A. *J. Chem. Phys.* **1998**, *109*, 5036.
- (7) Emberly, E. G.; Kirczenow, G. *Phys. Rev. B* **1998**, *58*, 10911.
- (8) Di Ventra, M.; Pantelides, S. T.; Lang, N. D. *Phys. Rev. Lett.* **2000**, *84*, 979.
- (9) Yaliraki, S. N.; Roitberg, A. E.; Gonzalez, C.; Mujica, V.; Ratner, M. A. *J. Chem. Phys.* **1999**, *111*, 6997.
- (10) Onipko, A.; Klymenko, Y.; Malysheva, L. *Phys. Rev. B* **2000**, *62*, 10480.
- (11) Nagoga, M.; Joachim, C. *Phys. Rev. B* **1997**, *56*, 4722.
- (12) Yaliraki, S. N.; Kemp, M.; Rantner, M. A. *J. Am. Chem. Soc.* **1999**, *121*, 3428.
- (13) Kornilovitch, P. E.; Bratkovsky, A. M. *Phys. Rev. B* **2001**, *64*, 195413.
- (14) Emberly, E. G.; Kirczenow, G. *Phys. Rev. Lett.* **2003**, *91*, 188301.
- (15) Lau, C. N.; Stewart, D. R.; Williams, R. S.; Bockrath, M. *Nano Lett.* **2004**, *4*, 569.

- (16) Nitzan, A.; Ratner, M. A. *Science* **2003**, *300*, 1384.
- (17) Tjernber, O.; Soderholm, S.; Karlsson, U. O.; Chiaia, G.; Qvarford, M.; Nysten, H.; Lindau, I. *Phys. Rev. B* **1996**, *53*, 10372.
- (18) Bjorneholm, O.; Nilsson, A.; Sandell, A.; Hermnas, B.; Martensson, N. *Phys. Rev. Lett.* **1992**, *68*, 1892.
- (19) Wurth, W.; Menzel, D. *Chem. Phys.* **2000**, *251*, 141.
- (20) Schnadt, J.; Bruhwiler, P. A.; Pattthey, L.; O'Shea, J. N.; Sodergren, S.; Odellius, M.; Ahuja, R.; Karis, O.; Bassler, M.; Persson, P.; Siegbahn, H.; Lunell, S.; Martensson, N. *Nature* **2002**, *418*, 620.
- (21) Fohlisch, A.; Feulner, P.; Hennies, F.; Fink, A.; Menzel, D.; Sanchez-Portal, D.; Echenique, P. M.; Wurth, W. *Nature* **2005**, *436*, 373.
- (22) Bruhwiler, P. A.; Karis, O.; Martensson, N. *Rev. Mod. Phys.* **2002**, *74*, 703.

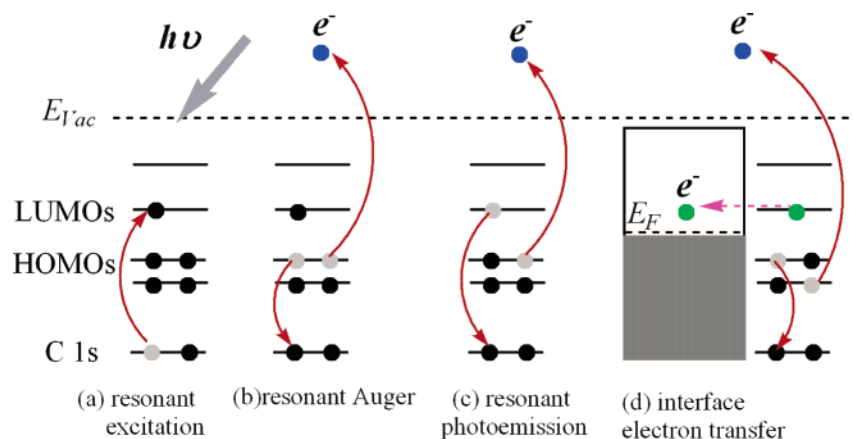


**Figure 1.** Schematic overview of the working principle of the resonant photoemission spectroscopy. (a) A core level electron (C 1s in our case) is resonantly excited into an adsorbate unoccupied molecular orbital (LUMO). In the core hole lifetime (6 fs for C 1s core hole), this excited electron can either be passive as a spectator (resonant Auger) (b) or participate in the decay process (resonant photoemission) (c), or directly transfer to the substrate conduction band if the molecular orbital strongly couples with substrate density of states (d) and the core hole is decayed via a normal Auger process.

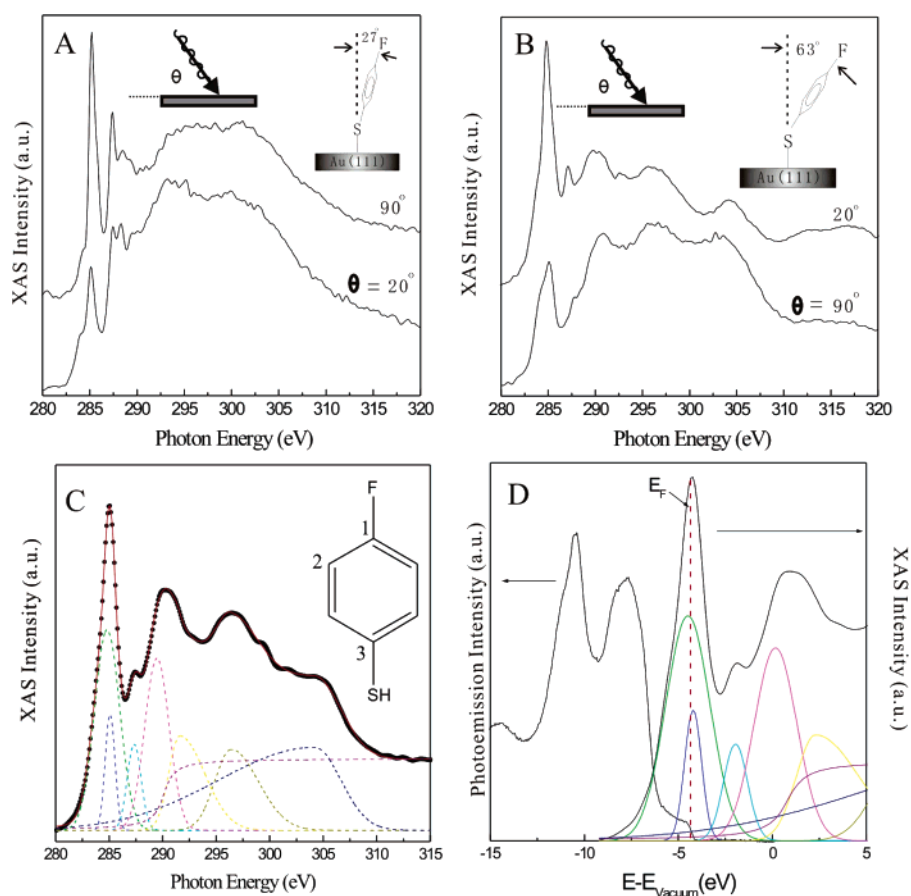


**Figure 2.** Polarization dependence of the XAS spectra (A) and (B) for samples A and B, respectively. (C) A fitting of the XAS spectrum for sample B taken at normal emission geometry. The black dot represents the raw data, and the red solid line is the best fit. The colorful dash lines denote the fitting components; see the text. (D) electronic structure of sample B. The Fermi level is derived from the Fermi edge of the underlying Au surface.

hole final state. The REPES signal intensity, which corresponds to the presence of resonant Auger and resonant photoemission transitions, can be used as an indicator to reflect the coupling strength between molecules and the Au substrate and reveals changes in the extent of localization of the molecular orbitals. Since no top metal electrode and electrical field are required, this measurement completely avoids the degradation of molecules and formation of metallic current paths that commonly occur in the metal/molecule/metal sandwich structure.

In this report, 4-fluorobenzenethiol/Au(111) is chosen as the test system since the molecule has a simple molecular structure (shown in the inset of Figure 2C) and unique  $\pi$ -orbitals (which leads to low barriers for electron transport<sup>23</sup>), and the substitution of a F atom induces the splitting of the absorption peak corresponding to the C 1s– $\pi^*$  transition<sup>24</sup> (discussed below). We show here that the electrons excited into the lowest

(23) Fischer, C. M.; Burghard, M.; Rothe, S. *Mater. Sci. Forum* **1995**, *191*, 149.

unoccupied molecular orbitals (LUMO) or LUMO+1 are strongly localized for molecules standing up on Au(111). In contrast, an ultrafast charge transfer process of  $<6$  fs is observed for molecules lying down on the surface. This configuration-dependent charge transfer process directly reflects the localization–delocalization transition of the molecular orbitals.

### Experimental Section

Two types of 4-fluorobenzenethiol monolayers were deposited on Au(111) substrates in solution or in vacuo. Clean Au(111) were obtained after cycles of Ar<sup>+</sup> sputtering and annealing at 450 °C. Sample A, a close-packed self-assembled monolayer of 4-fluorobenzenethiol molecules on Au(111), was formed by immersing a pre-cleaned Au(111) substrate into 3 mL of a  $1 \times 10^{-4}$  M solution in a N<sub>2</sub> environment for 48 h, using tetrahydrofuran (THF) as solvent. After the growth, the sample was thoroughly rinsed in THF and then immediately transferred into an ultrahigh vacuum (UHV) chamber with a base pressure of  $1.0 \times 10^{-10}$  Torr. Sample B was obtained by directly evaporating the molecules onto clean Au(111) in an ultrahigh vacuum chamber. During the evaporation, the chamber pressure rose to  $2.0 \times 10^{-6}$  Torr and Au(111) was held at room temperature. The sample was annealed at 60 °C immediately after the deposition. Due to the presence of S–Au bonds at the first monolayer, molecules in the multilayer desorbed after annealing leaving a self-assembled monolayer on Au(111).

The photoemission and X-ray absorption experiments were performed at the SINS beamline (photon energy 50–1200 eV) of the Singapore Synchrotron Light Source.<sup>25</sup> The X-ray absorption measurements were performed in total-yield mode with photon energy resolution of 0.1 eV. Resonant photoemission spectroscopy (REPES) intensities were normalized by the excitation light intensity. Binding energies for REPES were corrected by binding energy referencing the Au 4f<sub>7/2</sub> peak from Au(111).

### Results and Discussion

Figure 2A and 2B shows the C K-edge XAS spectra for samples A and B, respectively, at normal (90°) and glancing (20°) incidence. The ionization potential (IP) for the C 1s core level of the 4-fluorobenzenethiol monolayer on Au(111) is measured to be 290.36 eV by the cutoff method. The sharp absorption peaks in the C 1s XAS spectra below the IP are attributed to  $1s \rightarrow \pi^*$  resonances, and the broad peaks above the IP are ascribed to  $1s \rightarrow \sigma^*$  resonances. It is obvious from the polarization-dependent XAS spectra that samples A and B have different orientations on Au(111). In Figure 2A, the  $\pi^*$  resonances are enhanced at normal incidence ( $\theta = 90^\circ$ ), indicating that the molecular axis of the 4-fluorobenzenethiol molecule is closer to the vertical. The molecular tilt angle for sample A is calculated to be 27° (see inset of Figure 2A) using the formula given by J. Stohr.<sup>26</sup> On the other hand, the polarization dependence for sample B is reversed, indicating that the molecular axis is closer to the horizontal. The tilt angle for sample B is calculated to be 63°. The different molecular tilt angles for samples A and B are due to their different surface packing densities. The solution self-assembly method gives a higher packing density, causing the molecules to orientate more perpendicularly to the surface.

The C K-edge XAS spectra for samples A and B can be fitted with four Gaussian peaks corresponding to the C 1s– $\pi^*$  transition and three asymmetric C 1s– $\sigma^*$  transitions, as shown

in Figure 2C. The first three peaks located at 284.77, 285.07, and 287.27 eV are attributed to transitions from the C 1s core level to the lowest unoccupied molecular orbitals (LUMO). The different absorption resonances for the same transition originate from the different binding energies for C atoms at atomic sites 1, 2, and 3 shown in the inset of Figure 2C. The carbon at site 1 has the largest C 1s binding energy due to the large electronegativity of F.<sup>27</sup> The replacement of a H atom with a S atom at site 3 also shifts the binding energy of the carbon atom to higher energy compared to that of the remaining carbon atoms in the benzene ring. Careful least-squares fitting of the C 1s core level spectrum confirms the presence of three component peaks attributed to carbon atoms at different binding sites: C–H, C–S, and C–F. Therefore, the first three absorption resonances are attributed to the C 1s–LUMO transition at different atomic sites (the green curve for site 2, the blue for site 3, and the cyan for site 1). The fourth resonance (the purple curve) located at 289.37 eV is ascribed to the C 1s–LUMO+1 transition. We will address the C 1s–LUMO transition in a later section.

Figure 2D shows the electronic structure of 4-fluorobenzenethiol monolayers/Au(111) for sample B measured by the combination of the valence band spectrum taken at photon energy of 60 eV (left curve) and the C 1s XAS spectrum (right curve) using the same energy scale. The vacuum level is used as the common energy reference. The fitting components corresponding to the  $1s-\pi^*$  transitions at various atomic sites are also included in the XAS spectrum to show their positions relative to the Fermi level of the Au substrate. It is worth noting that the peak position of the resonance corresponding to the C 1s–LUMO transition for the carbon atom at site 2 (the green curve) is  $\sim 0.2$  eV below the Au Fermi level, and the peak position of the resonance for the carbon atom at site 3 (the blue curve) is just above the Fermi level. This is an effect of the core hole produced in XAS, which leads to energy shifts to higher binding energies.<sup>28</sup> However, the peak position of the resonance corresponding to the C 1s–LUMO transition for the carbon atom bonded to a F atom (the cyan curve) is much higher than the Fermi level ( $\sim 1.7$  eV higher). Similar relative positions to the Fermi level for the  $1s-\pi^*$  transitions at atomic sites are also observed in the combination of valence band spectrum and the XAS for sample A (not shown here).

Figure 3A and 3B shows the resonant photoemission (REPES) spectra as a contour plot across the C K-edge absorption region for samples A and B, respectively. The set of valence band spectra was recorded with incident photon energies ranging from 284 to 290 eV in steps of 0.2 eV, covering the C 1s–LUMO and C 1s–LUMO+1 resonances observed in the XAS spectra. In the REPES color scale, red denotes the strongest intensity and black corresponds to the weakest intensity. It is obvious that the REPES plot for sample A is significantly different from that for sample B. In sample A (molecules standing up on the surface), strong enhancements of the valence band can be clearly observed. The enhanced region (in yellow and orange) occurs at low binding energies in the valence band spectrum ( $\sim 2.5$  eV) and persists throughout the whole photon energy range used. On the other hand, for sample B (molecules lying down on the surface), much weaker enhancement of the valence electrons was observed, and the enhancement appears only at photon

(24) Hitchcock, A. P.; Fischer, P.; Gedanken, A.; Robin, M. B. *J. Phys. Chem.* **1987**, *91*, 531.

(25) Yu, X. J.; Wilhelm, O.; Moser, H. O.; Vidyarai, S. V.; Gao, X. Y.; Wee, A. T. S.; Nyurt, T.; Qian, H. J.; Zheng, H. W. *J. Electron Spectrosc. Relat. Phenom.* **2005**, *144*, 1031.

(26) Stohr, J. In *NEXAFS Spectroscopy*; Springer: Berlin, 1991; p 276.

(27) Chen, W.; Wang, L.; Huang, C.; Lin, T. T.; Gao, X. Y.; Loh, K. P.; Chen, Z. K.; Wee, A. T. S. *J. Am. Chem. Soc.* **2006**, *128*, 935.

(28) Persson, P.; Lunell, S.; Brühwiler, P. A.; Schnadt, J.; Sodergren, S.; O'Shea, J. N.; Karis, O.; Siegbahn, H.; Martensson, N.; Bässler, M.; Patthey, L. *J. Chem. Phys.* **2000**, *112*, 3945.

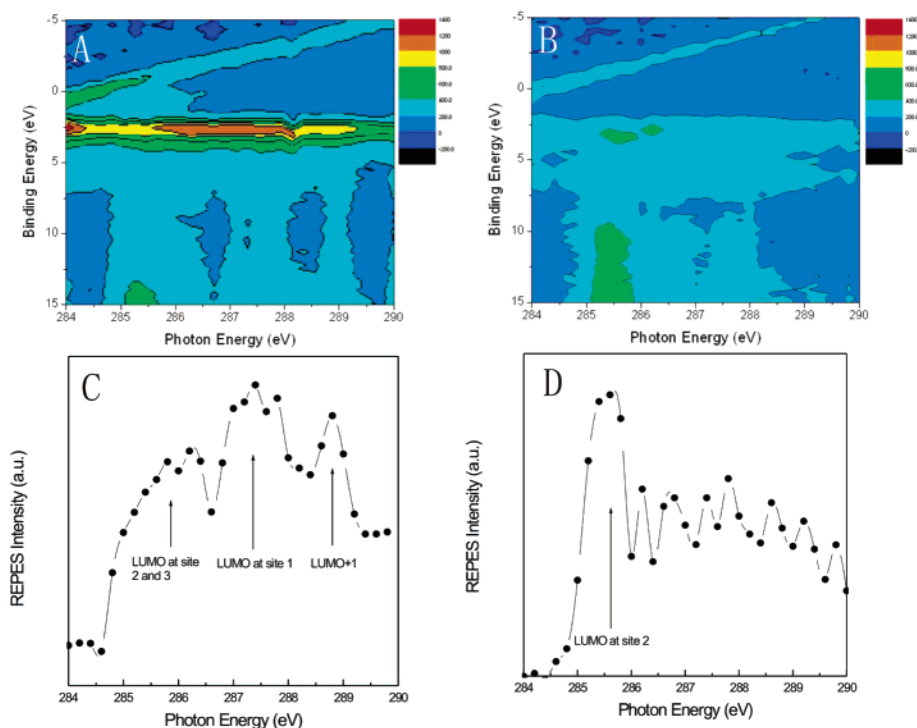


**Figure 3.** Resonant photoemission spectra (A) and (B) taken at the C K-edge region for samples A and B. Resonant signal (C) and (D) as a function of the photon energy for samples A and B.

energies around 285–286 eV. Note that the green part around the binding energy of 15 eV and the photon energy of 285–286 eV in both Figure 3A and B are due to the normal Auger decay processes.

To further elucidate the dependence of the valence electron enhancement on incident photon energy, the REPES intensities at various photon energies are obtained by subtracting the C 1s core level signal excited by second-order light (which appears near the Fermi level and its peak position increases with increasing photon energy) from the valence PES and then integrating the subtracted valence PES part at the region from 0 to 10 eV at corresponding photon energy. This allows one to probe the effect of exciting electrons from different core levels into the same unoccupied state or placing the excited electron into different unoccupied states. In Figure 3C, three peaks at 286.0, 287.4, and 288.8 eV are observed on the photon energy dependence curve of REPES intensity for sample A. The peaks correspond to the C 1s–LUMO transition for the carbon atoms at sites 2 and 3, the C 1s–LUMO transition for the carbon atom at site 1, and the C 1s–LUMO+1 transitions, respectively. The presence of these peaks indicates the opening of the resonant photoemission or resonant Auger channels during the deexcitation of the system and strongly suggests that, for sample A, the electrons excited from the C 1s core levels at various atomic sites into the LUMO or LUMO+1 orbitals are considerably localized during the lifetime of C 1s core hole. In contrast, only a peak at 285.6 eV is observed in the corresponding curve for sample B (Figure 3D). Moreover, this peak is much narrower than the corresponding peak in sample A. This peak corresponds to the C 1s–LUMO transition for the carbon atom at site 2. The disappearance of the peaks corresponding to the C 1s–LUMO for carbon atoms at sites 1 and 3 and the transition to the LUMO+1 indicate that, for sample B, strong interface charge transfer occurs before the core hole decay, in which the electrons excited into the unoccupied states rapidly delocalize

into the Au substrate. However, the charge transfer of the electrons excited from the C 1s core level to the LUMO for the carbon atoms at site 2 is energy-forbidden since the absorption resonance is  $\sim 0.2$  eV below the Fermi level of the gold substrate (Figure 2c). As a consequence, the REPES peak at 285.6 eV still remains for sample B. Similar energy-forbidden transitions have been observed in the LUMO in bi-isonicotinic acid on  $\text{TiO}_2$ .<sup>20</sup>

The molecules in sample A and B are connected to the gold substrate via S–Au bonds. The only difference between samples A and B is their molecular orientations: in sample A, the molecules stand up on the surface with a small tilt angle of  $27^\circ$ ; in sample B, the molecules lie down with a larger tilt angle of  $63^\circ$ . The fact that the interface charge transfer is present only in sample B indicates that the coupling between the molecules and the gold substrate is stronger with increasing molecular tilt angle. Previous work<sup>13,14</sup> theoretically demonstrates that the overlap between the molecular  $\pi$ -orbitals and the states of the contact is sensitive to the orientation of the molecule relative to the contacts and has a large effect on the conduction of the molecule. It is worth noting that the molecular orbitals are considered to be not strongly perturbed by the contact.<sup>13</sup> Interface charge transfer might take place via either or both of two pathways—adiabatic and nonadiabatic electron transfer. In the adiabatic mechanism, electron transfer occurs through a transition state. Nonadiabatic electron transfer involves direct quantum transitions between two localized states. Recently, Duncan et al.<sup>29</sup> studied the electron transfer process from alizarin chromophore into the  $\text{TiO}_2$  surface by ab initio nonadiabatic molecular dynamics. They concluded that the electron transfer in a system with strong molecule–substrate coupling is primarily adiabatic, while ultrafast transfer is indeed possible in the nonadiabatic mechanism. The adiabatic electron charge transfer

time is much shorter than that for the nonadiabatic process and can be as short as 3.2 fs in the case of the initial state above the conduction band of the substrate. Although the time for the charge transfer observed in sample B is difficult to estimate, it must be much less than the C 1s core hole lifetime (6 fs<sup>30</sup>) since the resonance peaks corresponding to the C 1s–LUMO transition for the carbon atoms at site 1 and the C 1s–LUMO+1 transitions are completely quenched. This suggests the transfer process observed here is dominated by the adiabatic electron transfer mechanism. The adiabatic mechanism is characterized by a change in the localization of molecular orbitals involved.<sup>29</sup> If electron transfer indeed occurs across the 4-fluorobenzenethiol/Au(111) interface, a localization–delocalization transition of the molecular orbitals is expected when the molecular orientation varies.

To understand the dependence of localization of the LUMO orbital of 4-fluorobenzenethiol monolayers on the tilting angle, we carried out first-principles density functional theory (DFT) calculations within the local density approximation (LDA). The SIESTA code was employed to solve the Kohn–Sham (KS) equations. The valence electrons are described by the linear combination of numerical atomic orbital basis set and the atomic core by norm-conserving Troullier–Martins pseudopotentials.<sup>31</sup> The double- $\zeta$  plus polarization atomic orbital basis set is employed in the calculation. The Hamiltonian matrix elements are calculated by charge density projection on a real space grid with an equivalent plane wave cutoff energy of 150 Ry.

Experiments and theoretical studies on self-assembled monolayers support that the hollow site is the preferred binding site.<sup>32,33</sup> Hence, the 4-fluorobenzenethiol molecules are assumed to bond to Au(111) at the hollow site, which was modeled by 7-atom Au clusters,<sup>34</sup> as shown in Figure 4a. For the molecules standing perpendicular to the metal surface, the perpendicular distances between the S atom and the Au surface is found to be about 2.19 Å after relaxing the 4-fluorobenzenethiol molecules on the 7-atom gold substrate, whose atomic positions are kept frozen to the bulk parameters (Au–Au = 2.88 Å). We allow the molecules to rotate about the terminal sulfur atoms while keeping the sulfur–gold bond length constant.<sup>13</sup> It is obvious that the LUMO distributions of 4-fluorobenzenethiol/Au(111) are dramatically changed at varying tilt angles, as shown in Figure 4b and 4c. For the molecule with a tilt angle of 27°, representing sample A, the LUMO orbitals distribute only around the molecules, consistent with previous reports.<sup>1,8</sup> In contrast, at a larger tilt angle of 63°, corresponding to sample B, a considerable portion of the LUMO is found to overlap on the Au substrate.

To understand quantitatively the orientation-induced orbital hybridization, the electron distributions of the LUMO states were calculated by Mulliken population analysis, as shown in Figure 4d. When the molecular tilt angle is smaller than 30°, the LUMO orbitals are completely localized within the molecule. With the

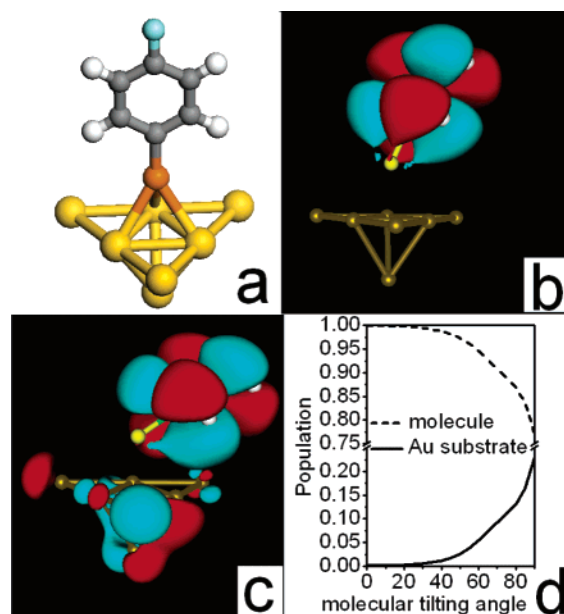


**Figure 4.** (a) Models of the 4-fluorobenzenethiol molecules bonded to Au(111) at the hollow site of 7-atom Au clusters. (b and c) Isosurface plots (isodensity value 0.01 au) of the LUMO orbitals for the molecules bonded to the Au(111) surface with tilt angles of 27 and 63°. (d) Mulliken population of the LUMO orbitals for the molecules bonded to the Au(111) surface with various molecular tilt angles.

increase of the tilt angle, the LUMO orbitals gradually spread across the molecule and are hybridized with the Au substrate. For the molecule with a tilt angle of 90°, corresponding to a completely flat molecule, about 30% of the LUMO state is delocalized from the molecule to the Au substrate due to the strong hybridization between the molecule and Au(111). A recent scanning tunneling microscopy study on linear chains of styrene and methylstyrene on Si(001) demonstrated that the coupling between the molecular orbitals of the benzene ring for styrene and the Si substrate becomes stronger as the molecule tilts more on the substrate.<sup>35</sup> In short, the molecular orbitals in the 4-fluorobenzenethiol/Au(111) interface experience a localization–delocalization transition when its orientation changes. This is consistent with our REPES experimental observations: ultrafast interfacial electron transfer is dominated by the adiabatic mechanism and only occurs when the delocalization of the LUMO orbitals opens a channel for the decay of excited electrons.

## Conclusion

In summary, interfacial charge transfer processes for 4-fluorobenzenethiol monolayers with different molecular orientations on Au(111) have been studied by resonant photoemission spectroscopy. An ultrafast charge transfer process was observed only for the molecules lying down on Au(111), when delocalization of the molecular orbitals to the Au substrate occurs. Theoretical calculations demonstrate that the molecular orbitals for a molecule bonded to Au(111) experience a localization–delocalization transition at larger molecular tilt angles resulting from hybridization between the molecular orbitals and metal. Thus, a simple molecule, such as 4-fluorobenzenethiol, can display bistable states that can be used as a molecular switch by simply controlling its orientation.

**Acknowledgment.** This work was supported by A\*STAR Grant No. R-144-000-106-305.

JA061741O

(29) Duncan, W. R.; Stier, W. M.; Prezhdo, O. V. *J. Am. Chem. Soc.* **2005**, *127*, 7941.

(30) Coville, M.; Thomas, T. D. *Phys. Rev. A* **1991**, *43*, 6053.

(31) Troullier, N.; Martins, J. L. *Phys. Rev. B* **1991**, *43*, 1993.

(32) Bumm, L. A.; Arnold, J. J.; Cygan, M. T.; Dunbar, T. D.; Burgin, T. P.; Jones, L., II; Allara, D. L.; Tour, J. M.; Weiss, P. S. *Science* **1996**, *271*, 1705.

(33) Beardmore, K. M.; Kress, J. D.; Gronbeck-Jense, N.; Bishop, A. R. *Chem. Phys. Lett.* **1998**, *286*, 40.

(34) Tulevski, G. S.; Myers, M. B.; Hybertsen, M. S.; Steigerwald, M. L.; Nuckolls, C. *Science* **2005**, *309*, 591.

(35) Kirczenow, G.; Piva, P. G.; Wolkow, R. A. *Phys. Rev. B* **2005**, *72*, 245306.